

2	Marc Pabst
3	Affiliation
4	Course Title
5	Professor Name
6	Due Date

7 Abstract

8 How does the brain process and represent successive sound in close temporal proximity? By
9 investigating mismatch negativity (MMN) components, prior research (Sussman & Gumenyuk,
10 2005; Sussman, Ritter & Vaughan, 1998) has suggested that temporal proximity plays an
11 important role in how sounds are represented in auditory memory. Here, we investigate how
12 predictability affects the election of mismatch negativity components in auditory sequences
13 consisting of two tones (frequent tone A = 440 Hz, rare tone B = 494 Hz, fixed SOA 100 ms).
14 In the predictable condition, tones are presented in a fixed order whereas in the unpredictable
15 condition, standards and deviants are presented in a pseudo-random order. We expect to find
16 that B tones in the unpredictable condition will elicit a significant MMN while B tones in the
17 predictable conditions will not. A repeating five-tone pattern was presented at several
18 stimulus rates (200, 400, 600, and 00 ms onset-to-onset) to determine at what temporal
19 proximity the five-tone repeating unit would be represented in memory. The mismatch
20 negativity component of event-related brain potentials was used to index how the sounds were
21 organized in memory when participants had no task with the sounds. Only at the 200-ms
22 onset-to-onset pace was the five-tone sequence unitized in memory. At presentation rates of
23 400 ms and above, the regularity (a different frequency tone occurred every fifth tone) was not
24 detected and mismatch negativity was elicited by these tones in the sequence. The results
25 show that temporal proximity plays a role in unitizing successive sounds in auditory memory.
26 These results also suggest that global relationships between successive sounds are represented
27 at the level of auditory cortices.

Revisiting the Stimulation-Rate-Dependent Pattern Mismatch Negativity

30

Abstract 2

Revisiting the Stimulation-Rate-Dependent Pattern Mismatch Negativity 3

Introduction 3

ASA 4

Hypothesis 6

Predictive Coding 8

Methods and Materials 9

Data Acquisition 9

Participants 9

Stimuli 9

Data Acquisition 10

Analysis Pipeline 11

Statistical Analysis 12

Standard Repetition Effects 12

MMN 12

Results 14

References 17

Introduction

How does the mind organize sequences of auditory stimuli?

At every moment, a rich spectro-temporal mixture of sounds hits our eardrums and causes the cochlea to vibrate, where stereocilia convert the vibrations into electrical impulses that race through the vestibulocochlear nerve to the primary auditory cortex. This part of the

53 hearing process is well understood but

54 **ASA**

55 How are these mere electrical signals processed, combined and finally formed into meaningful
56 perceptual experiences? While similar questions in the visual domain have intrigued scientists
57 for a very long time and most notably lead to the emergence of the Gestalt psychology in the
58 early 20th century, long before the term auditory scene analysis was coined. While the Gestalt
59 psychologists formulated very abstract rules, which in their own view should not be limited to
60 the visual domain but rather represent universal laws of human perception, their research was
61 almost exclusively carried out in the field of visual perception. Mainstream auditory perception
62 science was largely engaged in how very basic features of sound would connect to perception.
63 Particularly the works of A. Bregmann gave rise to a new framework called auditory scene
64 analysis. This proposed framework could serve a fundamental model of human auditory
65 perception and, in contrast to earlier approaches, could address questions of how humans are
66 able to form a coherent and meaningful representation of the auditory world. Bregman
67 suggests that the brain uses streaming and segregation to form auditory objects from
68 spectro-temporal information.

69 Auditory scene analysis thereby relies on two different categories of grouping, called
70 sequential and simultaneous integration. Simultaneous or vertical integration refers to the
71 grouping of concurrent properties into one or more separable auditory objects, a process
72 informed by temporal cues like common onset and offset, spectral and spatial characteristics
73 among others. Sequential integration on the other hand describes how temporally distinct
74 sounds are merged into one or multiple coherently perceived streams (contrary to simultaneous
75 grouping, only one such stream can be actively perceived at any time). While vertical and
76 horizontal grouping can come to different and therefore competing results (???), sequential
77 grouping often takes precedence over cues for simultaneous integration (???).

78 When presented with a series of similar or repeated auditory events, rare deviants
79 (termed oddballs) result in a negative deflection of event-related responses measured with EEG.
80 These alterations are indexed by the mismatch negativity (MMN) component obtained by
81 subtracting the response to deviant events from the response to standard events. Negativity is

strongest in the fronto-temporal area of the scalp with a peak latency ranging from 100 to 250 ms after stimulus onset. MMN components observed in magnetoencephalography (MEG) are called MMNm. There is a long line of research suggesting that MMN is pre-attentive (???). MMN has been traditionally described as an index of discrepancy between auditory input and the memory trace of the preceding standard stimuli (Paavilainen, 2013). The elicited MMN is not restricted to the repetition of physically identical stimuli but can also be observed when deviant events are of complex nature, e.g. when abstract auditory regularities are violated (Paavilainen, 2013). The regularities can come in the form of relationships between two tones (Saarinen et al. (1992) or multiple tones (Alain et al., 1994; Nordby et al., 1988; Schröger et al., 1996) and as with first-order MMNs could successfully be observed in infants (He et al., 2009).

Sussman et al. (1998) presented participants with a recurring five-tone pattern (A-A-A-A-B-A-A-A-A-B, '-' indicating silence between the tones). Differences in ERP following A and B tones were compared for rapid (SOA of 100 ms) and slow (SOA of 1200 ms) stimulation rates. MMN was only elicited, when stimuli were presented at a fast pace but no evidence was found at a SOA of 100 ms. In a subsequent study, Sussman & Gumenyuk (2005) used the same pattern at different SOA paces (200 ms, 400 ms, 800 ms). They also included a control condition in which tones presentation was pseudo-random (while keeping the probability of B tones at 20%). Similarly to their previous study, periodic presentation at 400 ms or slower stimulus-to-stimulus pace elicited a MMN, while at a stimulation rate of 200 ms such evidence was absent. They attributed this to competing predictive rules by which tones were either grouped sequentially or treated as distinct tones. Sussman et al. attributed this observation to sensory memory limitations, i.e., only when auditory memory could accommodate enough repetitions of the five-tone pattern tones could be integrated into a coherent representation and thereby allow the extraction of the underlying relationship.

1. replicated the procedure by Sussman et al. in an in-class setting.

- draw on the notion
-

Recently, the mismatch negativity has been described in the predictive coding framework.

A similar explanation can be offered in terms of predictive coding. Predictive coding is a biologically plausible model proposing prediction as the key feature of perception that was first described in the cortical visual system (Rao & Ballard, 1999). Taking a broader view, predictive coding is part of a research tradition taking a probabilistic (or Bayesian) approaches to brain function. Characterizing the brain as an *inference machine*, this line of reasoning traces back to Herman von Helmholtz's work in the late 19th century. In sharp contrast to traditional stimulus-driven models that describe the act of perception as a bottom-up process, in probabilistic terms, perception is not the direct result of sensory input, but is built by combining sensory input with predictions with internal, *probabilistic generative models*. Using prior knowledge about the world, these models are assumed to constantly create probabilistic versions of expected sensory input. Predictive coding more specifically suggests that at every processing state, predictions and actual input is constantly compared and only their difference, called *prediction error*, is propagated. Perception is thus seen as the process of improving the internal generative model by using sensory input to minimize prediction error. Because of that, predictive coding is sometimes casually referred to as *controlled hallucination*.

However, there are multiple in shortcoming in

Precision weighting

Hypothesis

As laid out above, we hypothesize that that two possible rules carry predictive value: Firstly, the presentation ratio of A and B tones (9 to 1) can be used to make proportion-dependent predictions as used in classical oddball-paradigms. When tones are presented in a regular fashion, as it is the case in the predictable condition, the extracted pattern might also be used to predict the next tone. Thus, two plausible but concurrent rules might guide predictions in the *predictable* condition, while in the *random* condition only the proportion-based regularity offers information to form predictions about upcoming tones. As has been shown before (???), pattern-based regularities are commonly found to take precedence over proportion-based regularities. If this is indeed the case, B-tones in the *predictable* condition should not be considered a *mismatch* and thus should not elicit a MMN. In contrast, since there is no way to predict B-tones in the *random* condition, these tones would be still considered as *deviant*

events and therefore expected to generate a MMN. Following this notion, one would also expect an expectation violation when predictable B-tones are replaced by A-tones, although they would be considered “standard” events when prediction is purely guided by proportion. This would be also in line with (Sussman et al., 1998; Sussman & Gumenyuk, 2005) interpretation of the original results.

pattern regularity

If the fixed order of the tones in the predictable state leads to a prediction of the B-tones, i.e. if the pattern regularity is extracted and the proportional regularity is irrelevant in the predictable context, we expect that the difference of predictable-BAAAAAA “B” and predictable-BAAA “A” is (significantly) less negative than the difference of random-BAAAAAA “B” minus random-BAAA “A”. In addition, we assume that the difference of predictable-BAAAA “B” and predictable-BAAA “A” is not significantly different from zero, while the difference of random-BAAAAAA “B” and random-BAAA “A” is significantly less than zero. In addition, in the predictable state, the interruption of the pattern regularity with an A tone should produce a significant negativity. This means that the difference between predictable-BAAAA “A” and predictable-BAAA “A” is significantly more negative than the difference between random-BAAAA “A” and random-BAAA “A”. In addition, we expect the difference between predictable-BAAAA “A” and predictable-BAAA “A” to be less than zero, while the difference between random-BAAAA “A” and random-BAAA “A” is not significantly different from zero.

, this process has been characterized as stimulus-driven

Predictive coding is a theoretical model based on the fundamental idea that

In this model, these predictions are what is actually perceived while sensory information is

- what are auditory objects?
- what influences their formation?
- what is predictive coding?
- how can objects be used for prediction?

168 • what happens when rules conflict?

169 • MMN and predictive coding?

170 **Predictive Coding**

171 • brain as inference machine

172 a. Auditory scene analysis

173 b. Sussman et al.

174 c. Scharf & Müller

175 d.

Methods and Materials

Data Acquisition

Participants

100 ms Presentation Rate Twenty-three psychology undergraduate students (2 males, average age 22.6 yrs., $SD = 5.57$, range 18 - 42 yrs.) were recruited at the Institute of Psychology at the University of Leipzig. All participants reported good general health, normal hearing and had normal or corrected-to-normal vision. Written informed consent was obtained before the experiment. One-third (34.8%) of participants spent time enaging in musical activities at time of survey, while 8.7% had no prior experience in music training. Handedness was asseced using a modified version of the Edinburgh Handedness Inventory (Oldfield, 1971, see appendix). A majoritiy (00%) of parcipitants favored the right hand. Participants were blinded in respect to the purpose of the experiment and received course credit in compensation.

150 ms Presentation Rate Twenty healthy participants (0 males, average age 00.0 yrs., $SD = 0.00$, range 00 - 00 yrs.) were recruited. Participants gave informed consent and reported normal hearing and corrected or corrected-to-normal vision. All participants were naive regarding the purpose of the experiment and were compensated in course credit or money. 00 participants (00%) had received musical training in the last 5 years before the experiment while 00 (00%) reported no musical experiance. In addition, participants reported if streaming occured during the presentation of the tones.

Stimuli

Stimuli consisted of pure sinusoidal tones with a duration of 50 ms (including a 10 ms cosine on/off ramp), presented isochronously at a stimulation onsets asynchrony (SOA) of 100 ms for study 1 and 150 ms for study 2. Participants where seated in a electromagnetically shielded and sound-proofed cabin while administering a total of 40 blocks containing a mixture of frequent 440 Hz tones (“A” tones) and infrequent 449 Hz tones (“B” tones). In one half of the blocks, tones were presented in pseudo-random order (e.g. A-A-A-B-A-B-A}, “random” condition), while in the remaining block tone presentation followed a simple pattern in which

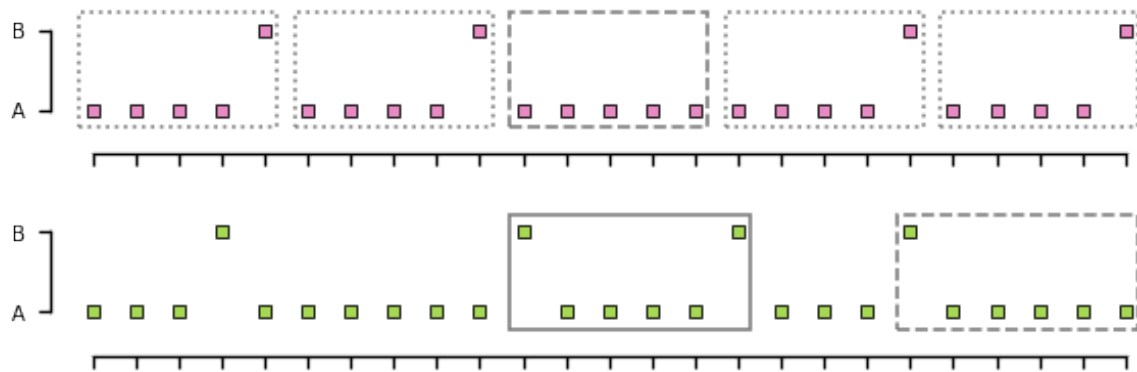


Figure 1. Tones of two different frequencies ($A=440$ Hz, $B=449$ Hz) were presented in two blocked conditions: In the “predictable” condition (top half), tones followed a simple pattern in which a single B-tone followed four A-tones. Some designated B-tones were replaced by A-tones (“pattern deviants”). In the “random” condition (lower half), tones were presented in a pseudo-random fashion ()

a five-tone-sequence of four frequent tones and one infrequent tone (i.e. A-A-A-A-B) was repeated cyclically (“predictable” condition). The ratio of frequent and infrequent tones was 10% for both conditions. Within the predictable condition, 10% of designated (infrequent) B tones were replaced by A tones, resulting in sporadic five-tone sequences consisting solely of A tones (i.e. A-A-A-A-A), thus violating the predictability rule. To assure comparability of local histories between tones in both conditions, randomly arranged tones were interspersed with sequences mimicking aforementioned patterns from the predictable condition (B-A-A-A-A-B and B-A-A-A-A-A) in the random condition. A grand total of 2000 tones in study 1 and 4000 tones in study 2 were delivered to each participant.

Data Acquisition

Electrophysiological data was recorded from active silver-silver-chloride ($Ag-AgCl$) electrodes using an ActiveTwo amplifier (BioSemi B.V., Amsterdam, The Netherlands). Acquisition was monitored online to ensure optimal data quality. A total of 39 channels were obtained using a 32-electrode-cap and 7 external electrodes. Scalp electrode locations conformed to the international 10–20 system. Horizontal and vertical eye movement was obtained using two bipolar configurations with electrodes placed around the lateral canthi of the eyes and above and below the right eye. Additionally, electrodes were placed on the tip of the nose and at the

left and right mastoid sites. Data was sampled at 512 Hz and on-line filtered at 1000 Hz.

Analysis Pipeline

Data preprocessing was implemented using a custom pipeline based on the *MNE Python* software package (Gramfort, 2013) using *Python 3.7*. All computations were carried out on a cluster operated by the University Computation Center of the University of Leipzig. Code used in thesis is publicly available at <https://github.com/marcpabst/xmas-oddballmatch>.

First, EEG data was subjected to the ZapLine procedure (de Cheveigné, 2020) to remove line noise contamination. A fivefold detection procedure as described by Bigdely-Shamlo et al. (2015) was then used to detect and subsequently interpolate bad channels. This specifically included the detection of channels that contain prolonged segments with very small values (i.e. flat channels), the exclusion of channels based on robust standard deviation (deviation criterion), unusually pronounced high-frequency noise (noisiness criterion), and the removal of channels that were poorly predicted by nearby channels (correlation criterion and predictability criterion). Channels considered bad by one or more of these methods were removed and interpolated using spherical splines (Perrin et al., 1989). Electrode locations for interpolations were informed by the BESA Spherical Head Model.

For Independent Component Analysis (ICA), data 1-Hz-high-pass filtered (134th order hamming-windowed FIR) was applied prior to ICA (Winkler et al., 2015). To further reduce artifacts, Artifact Subspace Reconstruction (ASR, Mullen et al., 2015) was used to identify parts of the data with unusual characteristics (bursts) which were subsequently removed. ICA was then carried out using the *Picard* algorithm (Ablin et al., 2018, 2017) on PCA-whitened data. To avoid rank-deficiency when extracting components from data with one or more interpolated channels, PCA was also used for dimensionality reduction. The EEGLAB (version 2020.0, Delorme & Makeig, 2004) software package and the IClab plugin (version 1.2.6, Pion-Tonachini et al., 2019) were used to automatically classify estimated components. Only components clearly classified (i.e. confidence above 50%) as resulting from either eye movement, muscular, or heartbeat activity were zeroed-out before applying the mixing matrix to unfiltered data.

In line with recommendations from Widmann et al. (2015) and de Cheveigné & Nelken

(2019), a ORDER finite impulse response (FIR) bandpass filter from 0.1 Hz to 30 Hz was applied in forward direction only (Hamming window with 0.0194 passband ripple and 53 dB stopband attenuation).

Continuous data was epoched into 400 ms long segments around stimulus onsets. Epochs included a 100 ms pre-stimulus interval. No baseline correction was applied. Segments exceeding a peak-to-peak voltage difference of 100 μ V were removed. No data set meet the pre-registered exclusion criterion stated of less than 100 trials per condition.

Statistical Analysis

Standard Repetition Effects

MMN

The dependent variable for analysing mismatch response was calculated by averaging amplitudes within a time window of ± 25 ms around the maximum negativity obtained by subtracting the mean ERP timecourse following the (expected) deviant event from the ERP following the (expected) standard event. To obtain mean amplitudes, ERPs to 4th position A tones (A-A-A-**A**-X, **boldface** indicates the tone of interest) and B tones (A-A-A-A-**B**) were averaged separately for both the *random* and the *predictable condition*. For the *random condition*, only tones that were part of a sequence mimicking the patterns from the predictable condition were included.

A three-way analysis of variance for repeated measures with the factors stimulus onset asynchrony (100 ms vs. 150 ms stimulus onset asynchrony), condition (predictable vs random presentation) and stimulus type (A tones vs. B tone).

To further analyse Following the pre-registration, a two-way analysis of variance for repeated measures to test for significant differences of mean amplitudes in the MMN window between standard and deviant tones (stimulus type) depending on the condition (predictable vs. random) was calculated separately for both 100 ms and 150 ms presentation. In line with Sussman & Gumenyuk (2005), FZ, F3, F4, FC1, and FC2 electrode locations were averaged. Greenhouse-Geisser correction for lack of sphericity was applied when appropriate.

For post-hoc comparison, two-tailed Student's t-test were calculated for . P-values

278 were corrected for multiple comparisons by using the Benjamini-Hochberg procedure.

Results

Grand averages of event-related potentials (ERP) at pooled FZ, F3, F4, FC1, and FC2 electrode locations to A tones (A-A-A-A-**X**), B tones (A-A-A-A-**B**), and their difference (**B** tone minus **A** tone) are displayed in Figure X for both 100 ms (left panel) and 150 ms (right panel) stimulus onset asynchronies. Top half of each panel shows ERPs in the *predictable condition* while lower half depicts ERPs in the *random condition*. For both presentation rates, clear rhythms matching the presentation frequency of 10 Hz (100 ms) and respectively 6.667 Hz (150 ms) are seen as a result from substantial overlap of neighboring tones. Panels also show the distribution of mean amplitude differences in the MMN latency window (as defined above, 110 ms to 160 ms after stimulus onset) across participants and the difference of scalp topographies averaged over the same interval. Similarly, waveforms and mean amplitude difference distributions at pooled mastoid sites are shown in Figure X.

Evoked responses to A and B tones were compared by calculating mean amplitudes in the MMN latency window. Mean amplitudes in the MMN latency window and their standard deviations (SD) for all conditions are shown in Table X. Descriptively, mean amplitudes at pooled fronto-central electrode locations were more negative for randomly presented B tones than for randomly presented A tones, regardless of tone presentation rate (100 ms: $\Delta M = -0.358 \mu V$; 150 ms: $\Delta M = -0.555 \mu V$) This also held true for tones presented in a predictable fashion, but for the slower of the two presentation rates only ($\Delta M = -0.582 \mu V$). In contrast, when predictable tone patterns occurred at a faster 100 ms rate, B tones elicited descriptively more positive responses than A tones ($\Delta M = 0.383 \mu V$). Descriptive comparison of evoked responses from pooled left and right mastoids revealed that pseudo-randomly presented B tones were more positive in the MMN latency window than A tones (100-ms-SOA: $\Delta M = 0.746 \mu V$, 150-ms-SOA: $\Delta M = 0.510 \mu V$). A similar observation could be made for predictable B tones compared to the preceding A tones at a SOA of 150 ms ($\Delta M = 0.399 \mu V$) but not for the faster presentation rate ($\Delta M = -0.132 \mu V$).

Statistical analyses provided support for these findings. For the 100 ms stimulation rate, the three-way ANOVA yielded a significant three-way interaction effect (*condition* x *stimulus type* x *electrode locations*; $F(1, 19) = 7.53$, $p = 0.0130$) but failed to reveal main effects for factors *stimulus type* ($F(1, 19) = 1.05$, $p = 0.3180$), *condition* ($F(1, 19) = 0.83$,

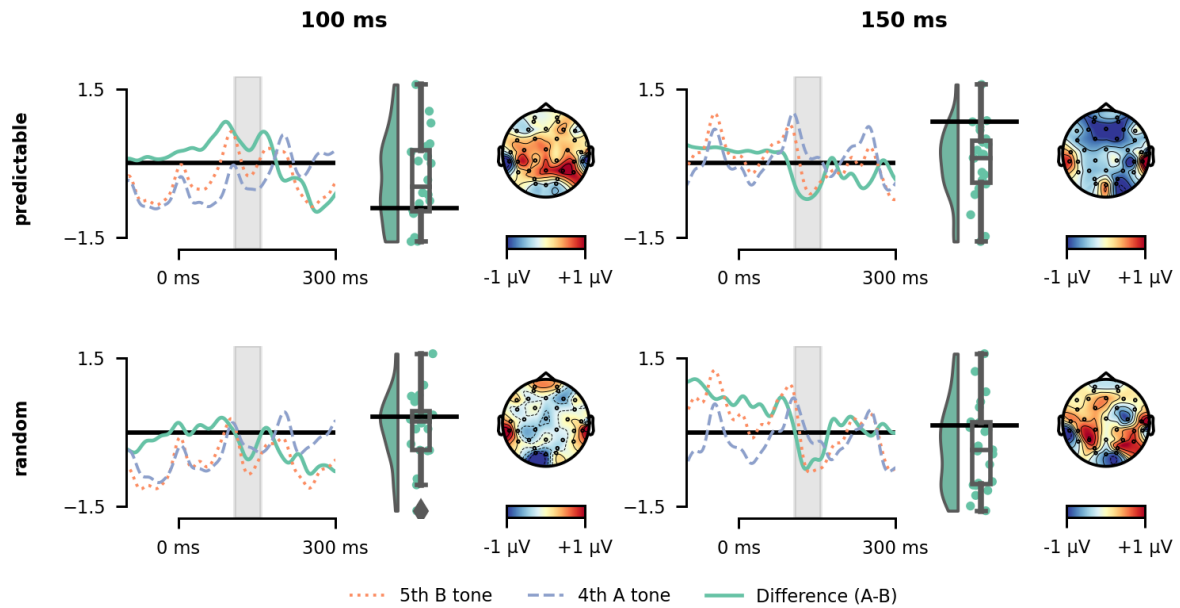


Figure 2. ERP grand averages (pooled FZ, F3, F4, FC1, and FC2 electrode locations) for an SOA of 100 ms (left) and 150 ms (right), for A tones (A-A-A-A-X, blue dashed lines) and B tones (A-A-A-A-B, orange dashed line) and their difference (B - A, green solid line). Upper panels show ERPs for tones presented in a predictable pattern (predictable condition) while lower panels show ERPs for tones presented in pseudo-random order (random condition). Shaded area marks MMN latency window (110 ms to 160 ms) used to calculate the distribution of amplitude differences across participants (middle of each panel) and the difference of topographic maps averaged over the same interval (right of each panel).

$p = 0.3730$), and electrode locations ($F(1, 19) = 0.04$, $p = 0.8520$). In contrast, for tones presented at a SOA of 150 ms only the two-way interaction term *stimulus type* x *electrode locations* had a significant effect ($F(1, 22) = 20.76$, $p = 0.0002$). Mean amplitudes in the MMN latency window however did not differ for factors *stimulus type* ($F(1, 22) = 0.32$, $p = 0.5790$), *electrode locations* ().

Two-way ANOVAs (*Condition* x *Stimulus Type*) were carried out separately for pooled fronto-central and mastoid electrode locations. For 100 ms tone presentation rate, the Condition x StimulusType interaction only revealed a significant effect for the fronto-central electrode cluster ($F(1, 19) = 16.75$, $p = 0.0006$) but not for pooled mastoid sites ($F(1, 19) = 2.37$, $p = 0.1410$) indicating that the 3-way interaction effect condition x stimulus type x electrode is indeed driven by the amplitude differences in the fronto-central electrode

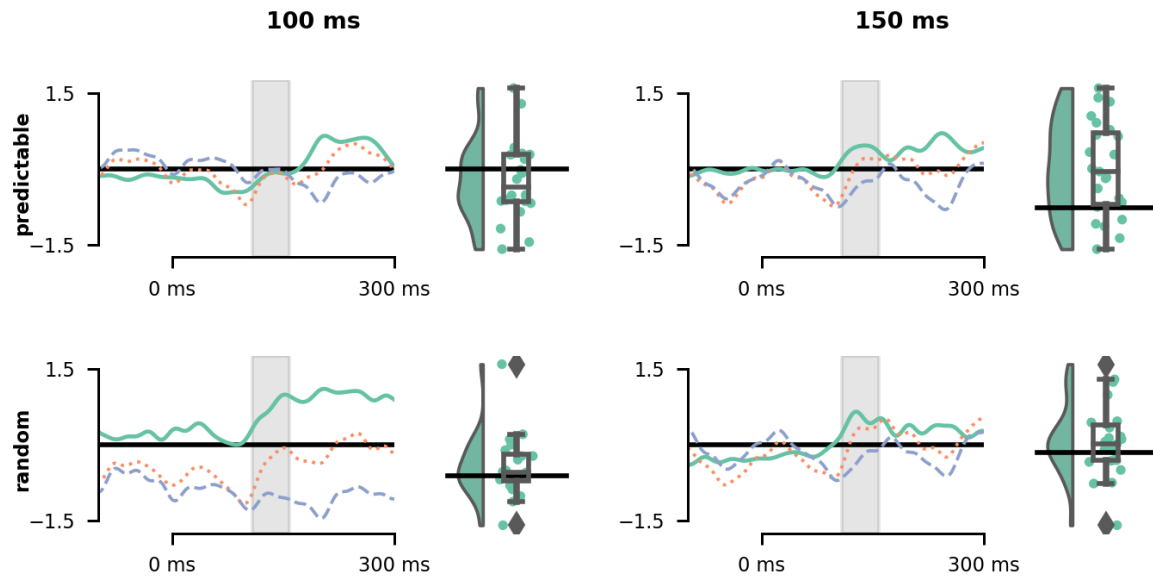


Figure 3. ERP grand averages (pooled M1, M2 electrode locations) for an SOA of 100 ms (left) and 150 ms (right), for A tones (A-A-A-A-X, blue dashed lines) and B tones (A-A-A-A-B, orange dashed line) and their difference (B - A, green solid line). Upper panels show ERPs for tones presented in a predictable pattern (predictable condition) while lower panels show ERPs for tones presented in pseudo-random order (random condition). Shaded area marks MMN latency window (110 ms to 160 ms) used to calculate the distribution of amplitude differences across participants.

locations . Contrary to this, for the 150 ms presentation rate, main effects for *stimulus type* were significant for both fronto-central and mastoid sites, suggesting that there was both a MMN at fronto-central locations as well as a polarity-reversal at the mastoid electrodes.

For the 150 ms stimulation rate, the 2-way ANOVA yielded a significant main effect for stimulus type ($F(1, 22) = 22.67, p = 0.0001$) but not for condition ($F(1, 22) = 0.95, p = 0.3410$) or stimulus type x condition interaction ($F(1, 22) = 0.03, p = 0.8680$). In contrast, when presenting tones with a stimulus-onset-asyncrny of 100 ms, no such effects were found for the factor condition ($F(1, 22) = 0.95, p = 0.3410$), stimulus type ($F(1, 22) = 22.67, p = 0.0001$), or interaction ($F(1, 22) = 0.03, p = 0.8680$).

Figure X shows EEG waveform averages (pooled FZ, F3, F4, FC1, and FC2 electrode locations) for five-tone sequences (A-A-A-A-B) presented in a *predictable* (top panel) and *random* contexts (lower panel).

SOA	Condition	StimulusType	Mean	SD	Mean	SD
100	predictable	A	-0.431	1.23	-0.052	1.51
		B	-0.0477	1.22	-0.184	1.56
	random	A	-0.225	1.82	-1.04	2.64
		B	-0.583	2.16	-0.296	3.23
150	predictable	A	0.25	0.967	-0.349	1.19
		B	-0.331	1.09	0.0492	1.33
	random	A	0.0233	1.75	-0.292	1.64
		B	-0.531	1.82	0.218	2.38

References

- MMN explained by positiviy (?) -> first-order MMN?
- Ablin, P., Cardoso, J.-F., & Gramfort, A. (2018). Faster independent component analysis by preconditioning with Hessian approximations. *IEEE Transactions on Signal Processing*, 66(15), 4040–4049. <https://doi.org/10.1109/TSP.2018.2844203>
- Ablin, P., Cardoso, J.-F., & Gramfort, A. (2017). Faster ICA under orthogonal constraint. *arXiv:1711.10873 [Stat]*. <http://arxiv.org/abs/1711.10873>
- Alain, C., Woods, D. L., & Ogawa, K. H. (1994). Brain indices of automatic pattern processing: *NeuroReport*, 6(1), 140–144. <https://doi.org/10.1097/00001756-199412300-00036>
- Bigdely-Shamlo, N., Mullen, T., Kothe, C., Su, K.-M., & Robbins, K. A. (2015). The PREP pipeline: standardized preprocessing for large-scale EEG analysis. *Frontiers in Neuroinformatics*, 9. <https://doi.org/10.3389/fninf.2015.00016>
- de Cheveigné, A. (2020). ZapLine: A simple and effective method to remove power line artifacts. *NeuroImage*, 207, 116356. <https://doi.org/10.1016/j.neuroimage.2019.116356>
- de Cheveigné, A., & Nelken, I. (2019). Filters: When, Why, and How (Not) to Use Them. *Neuron*, 102(2), 280–293. <https://doi.org/10.1016/j.neuron.2019.02.039>

Table 1

Results of the 3-way ANOVA (condition x stimulus x electrode) for repeated measures conducted on the mean ERP-amplitudes (time window 111 - 161 ms) at electrode Fz (upper section). The significant interaction between the three factors included was further analyzed by 2-way ANOVAS (stimulus x electrode) conducted separately for the random condition (middle section) and the predictable condition (lower section).

	Effect	DFn	DFd	F	p	p<.05	ges
100 ms	Condition	1	19	0.831	0.373		0.008
	StimulusType	1	19	1.05	0.318		0.002
	Electrode	1	19	0.036	0.852		0.000331
	Condition x StimulusType	1	19	0.051	0.823		7.55e-05
	Condition x Electrode	1	19	0.763	0.393		0.002
	StimulusType x Electrode	1	19	0.797	0.383		0.001
	Condition x StimulusType x Electrode	1	19	7.53	0.013	*	0.01
150 ms	Condition	1	22	0.08	0.78		0.000263
	StimulusType	1	22	0.317	0.579		0.000339
	Electrode	1	22	0.035	0.854		0.000301
	Condition x StimulusType	1	22	0.16	0.693		0.000124
	Condition x Electrode	1	22	1.13	0.299		0.003
	StimulusType x Electrode	1	22	20.8	0.000155	*	0.026
	Condition x StimulusType x Electrode	1	22	0.053	0.819		4.63e-05

349 Delorme, A., & Makeig, S. (2004). EEGLAB: an open source toolbox for analysis of
 350 single-trial EEG dynamics including independent component analysis. *Journal of*
 351 *Neuroscience Methods*, 134(1), 9–21. <https://doi.org/10.1016/j.jneumeth.2003.10.009>

352 Gramfort, A. (2013). MEG and EEG data analysis with MNE-Python. *Frontiers in*
 353 *Neuroscience*, 7. <https://doi.org/10.3389/fnins.2013.00267>

354 He, C., Hotson, L., & Trainor, L. J. (2009). Development of infant mismatch responses to
 355 auditory pattern changes between 2 and 4 months old. *European Journal of Neuroscience*,
 356 29(4), 861–867. <https://doi.org/10.1111/j.1460-9568.2009.06625.x>

Table 2

Results of the 3-way ANOVA (condition x stimulus x electrode) for repeated measures conducted on the mean ERP-amplitudes (time window 111 - 161 ms) at electrode Fz (upper section). The significant interaction between the three factors included was further analyzed by 2-way ANOVAS (stimulus x electrode) conducted separately for the random condition (middle section) and the predictable condition (lower section).

		Effect	DFn	DFd	F	p	p<.05	ges
100 ms	Frontal	Condition	1	19	0.16	.694		0.003
		StimulusType	1	19	0.006	.938		1.5e-05
		Condition x StimulusType	1	19	16.7	<.001	*	0.013
	Mastoids	Condition	1	19	1.28	.272		0.014
		StimulusType	1	19	1.21	.285		0.004
		Condition x StimulusType	1	19	2.37	.141		0.009
150 ms	Frontal	Condition	1	22	0.947	.341		0.006
		StimulusType	1	22	22.7	<.001	*	0.038
		Condition x StimulusType	1	22	0.028	.868		2.2e-05
	Mastoids	Condition	1	22	0.206	.655		0.001
		StimulusType	1	22	6.56	.018	*	0.018
		Condition x StimulusType	1	22	0.122	.730		0.00028

Mullen, T. R., Kothe, C. A. E., Chi, Y. M., Ojeda, A., Kerth, T., Makeig, S., Jung, T.-P., & Cauwenberghs, G. (2015). Real-time neuroimaging and cognitive monitoring using wearable dry EEG. *IEEE Transactions on Biomedical Engineering*, 62(11), 2553–2567. <https://doi.org/10.1109/TBME.2015.2481482>

Nordby, H., Roth, W. T., & Pfefferbaum, A. (1988). Event-Related Potentials to Breaks in Sequences of Alternating Pitches or Interstimulus Intervals. *Psychophysiology*, 25(3), 262–268. <https://doi.org/10.1111/j.1469-8986.1988.tb01239.x>

Oldfield, R. C. (1971). The assessment and analysis of handedness: the Edinburgh inventory. *Neuropsychologia*, 9(1), 97–113. [https://doi.org/10.1016/0028-3932\(71\)90067-4](https://doi.org/10.1016/0028-3932(71)90067-4)

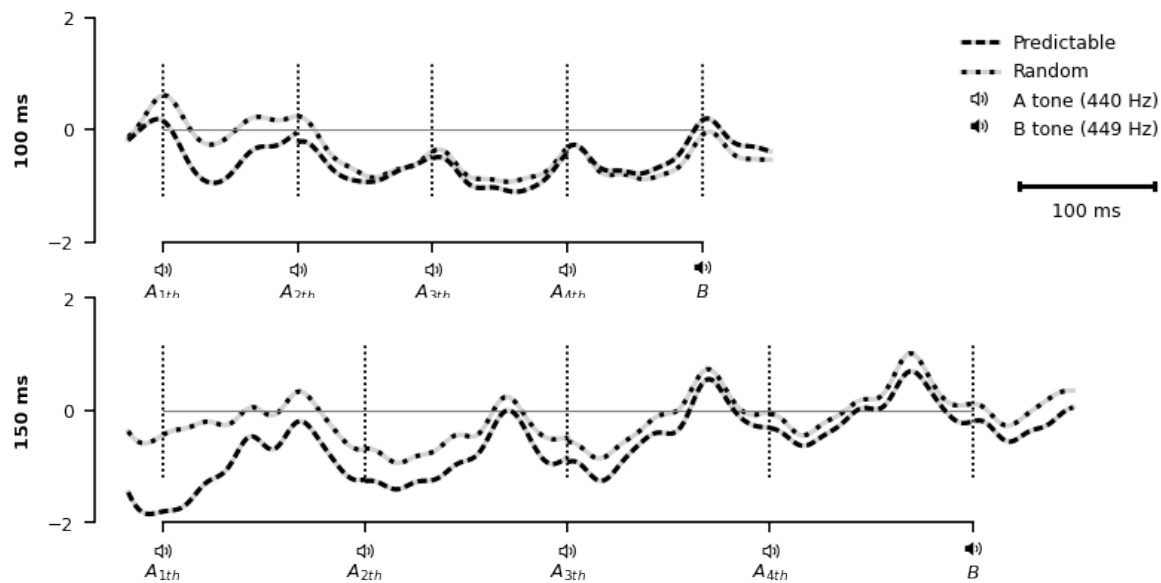


Figure 4. EEG waveforms for five-tone sequences presented in an predictable context (dotted line) and pseudo-random condition (dashed line) for 100 ms presentation rate (top panel) and 150 ms presentation rate (lower panel). Vertical lines indicate tone onset.

- Paavilainen, P. (2013). The mismatch-negativity (MMN) component of the auditory event-related potential to violations of abstract regularities: A review. *International Journal of Psychophysiology*, 88(2), 109–123. <https://doi.org/10.1016/j.ijpsycho.2013.03.015>
- Perrin, F., Pernier, J., Bertrand, O., & Echallier, J. F. (1989). Spherical splines for scalp potential and current density mapping. *Electroencephalography and Clinical Neurophysiology*, 72(2), 184–187. [https://doi.org/10.1016/0013-4694\(89\)90180-6](https://doi.org/10.1016/0013-4694(89)90180-6)
- Pion-Tonachini, L., Kreutz-Delgado, K., & Makeig, S. (2019). ICLabel: An automated electroencephalographic independent component classifier, dataset, and website. *NeuroImage*, 198, 181–197. <https://doi.org/10.1016/j.neuroimage.2019.05.026>
- Rao, R. P. N., & Ballard, D. H. (1999). Predictive coding in the visual cortex: a functional interpretation of some extra-classical receptive-field effects. *Nature Neuroscience*, 2(1), 79–87. <https://doi.org/10.1038/4580>

- Saarinen, J., Paavilainen, P., Schöger, E., Tervaniemi, M., & Näätänen, R. (1992). Representation of abstract attributes of auditory stimuli in the human brain: *NeuroReport*, 3(12), 1149–1151. <https://doi.org/10.1097/00001756-199212000-00030>
- Schröger, E., Tervaniemi, M., Wolff, C., & Näätänen, R. N. (1996). Preattentive periodicity detection in auditory patterns as governed by time and intensity information. *Cognitive Brain Research*, 4(2), 145–148. [https://doi.org/10.1016/0926-6410\(96\)00023-7](https://doi.org/10.1016/0926-6410(96)00023-7)
- Sussman, E., Ritter, W., & Vaughan, H. G. (1998). Predictability of stimulus deviance and the mismatch negativity: *NeuroReport*, 9(18), 4167–4170. <https://doi.org/10.1097/00001756-199812210-00031>
- Sussman, E. S., & Gumenyuk, V. (2005). Organization of sequential sounds in auditory memory: *NeuroReport*, 16(13), 1519–1523. <https://doi.org/10.1097/01.wnr.0000177002.35193.4c>
- Widmann, A., Schröger, E., & Maess, B. (2015). Digital filter design for electrophysiological data – a practical approach. *Journal of Neuroscience Methods*, 250, 34–46. <https://doi.org/10.1016/j.jneumeth.2014.08.002>
- Winkler, I., Debener, S., Müller, K.-R., & Tangermann, M. (2015). On the influence of high-pass filtering on ICA-based artifact reduction in EEG-ERP. *2015 37th Annual International Conference of the IEEE Engineering in Medicine and Biology Society (EMBC)*, 4101–4105. <https://doi.org/10.1109/EMBC.2015.7319296>